monocytosis or increased HbF. Detailed clinical history and laboratory data is provided as Supplemental data 1.

Detailed methods for experiments are described in Supplemental data 2

Results and Discussion

Case 1 showed a high likelihood of being a case of ALPS according to the symptoms and clinical data presented (Supplemental data 1, Table 1) except for number of Double-negative T (DNT) cells which was only 1.4% of TCRαβ cells (Fig. 1a). JMML was also nominated as a disease to be differentiated, because remarkable hepatosplenomegaly with thrombocythemia and moderate monocytosis was noted. However, no hypersensitivity to GM-CSF as determined by colony formation assay for BM-MNC (data not shown) or phospho STAT5 staining (data not shown) was observed. DNA sequence for JMML associated genes such as *NRAS, KRAS, HRAS, PTPN11* and *CBL* was determined, and KRAS G13D mutation was identified (Fig. 1b). The mutation was seen exclusively in the hematopoietic cell lineage and no mutation was seen in the oral mucosa or nail-derived DNA. Granulocytes, monocytes, T cells, and B cells were all positive for KRAS G13D mutation (data not shown). The proportion of mutated cells in each hematopoietic lineage was quantitated by mutation allele specific quantitative PCR methods, which revealed mutated allele was almost equally present in granulocytes, T cells and B cells (Fig 1c). CD34-positive hematopoietic stem cells (HSC) was also positive for KRAS G13D mutation, and 60% of CFU-GM colonies developed from isolated CD34 cells carried KRAS G13D mutation (data not shown). These observations suggest that the mutation occurred at the HSC level, and HSCs consists of wild type and mutant HSCs.

NRAS mutated Type IV ALPS was previously characterized by apoptosis

resistance of T-cells in IL-2 depeletion[3]. Then, activated T cells were subjected to an apoptosis assay by FAS stimulation or IL-2 depletion. Remarkable resistance to IL-2 depletion but not to FAS-dependent apoptosis (Fig. 1d and e) was seen. This was in contrast to T cells from FAS mutated ALPS type 1a which showed remarkable resistance to FAS dependent apoptosis and normal apoptosis induction by IL-2 withdrawal (Fig. 1d and e). Western blotting analysis of activated T cells or Epstein-Barr virus-transformed B cells showed reduced expression of Bim (Fig. 1f).

In case 2, autoimmune phenotype and hepatosplenomegaly were remarkable as shown in Supplementary data 1. The patient was initially diagnosed as Evans Syndrome based on presence of hemolytic anemia and autoimmune thrombocytopenia. DNT cells were 1.1% of TCRαβ cells in the peripheral blood, which did not meet with the criteria of ALPS. Although spontaneous colony formation was shown in PB- and BM-MNC, and GM-CSF hypersensitivity was demonstrated in BM-MNC derived CD34 positive cell (Supplemental data 1 Table2), she showed no massive monocytosis or increased HbF. Thus the diagnosis was less likely to be ALPS or JMML. DNA sequencing of JMML related genes such as *NRAS, KRAS, HRAS, PTPN11*, and *CBL* identified somatic but not germline KRAS G13D mutation (Fig. 1b). KRAS G13D mutation was detected in granulocytes and T cells. Mutation was not identified in B cells by conventional DNA sequencing (data not shown). Mutant allele specific quantitative PCR revealed mutated allele was almost equally present in granulocytes and T cells, but barely in B cells (Fig. 1c). Activated T cells showed resistance to IL-2 depletion but not to FAS-dependent apoptosis (Fig. 1d and e). Both of our cases were characterized by strong autoimmunity, immune cytopenia and lymphadenopathy or hepatosplenomegaly with partial similarity with ALPS or JMML. However, they did not meet with the well defied diagnostic

criteria of ALPS[2] or JMML[6]. It is interesting that Case 2 presented GM-CSF hypersensitivity, which is one of the hallmarks of JMML. Given the strict clinical and laboratory criteria of JMML and ALPS, our two cases should be defined as a new disease entity, like RAS associated ALPS like disease (RALD). Recently defined NRAS mutated ALPS type IV may also be included in a similar disease entity.

There are several cases of JMML reported simultaneously having clinical and laboratory findings compatible with autoimmune disease[8,9]. Autoimmune syndromes are occasionally seen in patients with myelodysplastic syndromes, including chronic myelomonocytic leukemia[10]. These previous findings may suggest a close relationship of autoimmune disease and JMML. Since KRAS G13D has been identified in JMML[11-13], it is tempting to speculate that KRAS G13D mutation is involved in JMML as well as RAS associated ALPS like disease (RALD). It should be noted in JMML, erythroid cells reportedly carry mutant RAS, while B and T cell involvement was variable[13]. In both of our cases, myeloid cells and T cells carried mutant RAS, while B cells were affected variably. These findings would support a hypothesis that the clinical and hematological features are related to the differentiation stages of hematopoietic stem cells where RAS mutation is acquired. JMML-like myelo-monocytic proliferation may predict an involvement of RAS mutation in myeloid stem/precursor cell level whereas ALPS-like phenotype may predict that of stem/precursor cells of lymphoid lineage, especially of T cells. Under the light of subtle differences between the two cases presented, their hematological and clinical features may reflect the characteristics of the stem cell level where *KRAS* mutation is acquired. Involvement of the precursors with higher propensity toward lymphoid lineage may lead to autoimmune phenotypes, while involvement of those with propensity toward the myeloid lineage may lead to GM-CSF hypersensitivity while still

sharing some overlapping autoimmune characteristics.

One may argue from the other points of view with regard to the clinicopathological features of these disorders. First, transformation in a fetal HSC might be obligatory for the development of JMML[14] and that in HSC later in life may not have the same consequences. Second, certain KRAS mutations may be more potent than the others. Codon 13 mutations are generally less deleterious biochemically than codon 12 substitutions, and patients with JMML with codon 13 mutations have been reported to show spontaneous hematologic improvement[12,15]. Thus further studies are needed to reveal in-depth clinicopathological characteristics in this type of lympho-myelo proliferative disorders.

KRAS mutation may initiate the oncogenic pathway as one of the first genetic hits, but is insufficient to cause frank malignancy by itself[16,17]. Considering recent findings that additional mutations of the genes involved in DNA repair, cell cycle arrest, and apoptosis are required for full malignant transformation, one can argue that RAS associated ALPS like disease (RALD) patients will also develop malignancies during the course of the diseases. Occasional association of myeloid blast crisis in JMML and that of lymphoid malignancies in ALPS will support this notion. Thus the two patients are now being followed up carefully. It was recently revealed that half of the patients diagnosed with Evans syndrome, an autoimmune disease presenting with hemolytic anemia and thrombocytopenia, meet the criteria for ALPS diagnosis[18,19]. In this study, FAS-mediated apoptosis analysis was utilized for the screening. Considering the cases we presented, it will be intriguing to re-evaluate Evans syndrome by IL-2 depletion-dependent apoptosis assay focusing on the overlapping autoimmunity with RAS associated ALPS like disease (RALD).

Acknowledgements

This work was supported by a Grant-in-Aid from the Ministry of Education, Science, and Culture, 20390302 (Japan) for SM and by a Grant-in-Aid for Cancer Research from the Ministry of Health, Labor and Welfare, 20-4 and 19-9 (Japan) for SM and MT.

Author ship

MT and SM designed entire experiments and wrote this manuscript. KS, NM, and MT treat those patients, and designed clinical laboratory test. JP performed experiments described in Fig.1b-f. KM, HM, and SD performed colony and mutational analysis. MN, TM, KK, SK, YK and AT supervised clinical and immunological experiments, or coordinated clinical information.

Conflict of interest disclosure

The authors declare no conflict of interest.

References

1. Fisher GH, Rosenberg FJ, Straus SE, et al. Dominant interfering Fas gene mutations impair apoptosis in a human autoimmune lymphoproliferative syndrome. *Cell*. 1995;81(6):935-946.

2. Teachey DT, Seif AE, Grupp SA. Advances in the management and understanding of autoimmune lymphoproliferative syndrome (ALPS). *Br J Haematol*.148(2):205-216.

3. Oliveira JB, Bidere N, Niemela JE, et al. NRAS mutation causes a human autoimmune lymphoproliferative syndrome. *Proc Natl Acad Sci U S A*. 2007;104(21):8953-8958.

4. Oliveira J, Bleesing J, Dianzani U, et al. Revised diagnostic criteria and classification for the autoimmune lymphoproliferative syndrome (ALPS): report from the 2009 NIH International Workshop. *Blood*. 2010;116(14):e35-e40.

5. Miyauchi J, Asada M, Sasaki M, Tsunematsu Y, Kojima S, Mizutani S. Mutations of the N-ras gene in juvenile chronic myelogenous leukemia. *Blood*. 1994;83(8):2248-2254.

6. Emanuel PD. Juvenile myelomonocytic leukemia and chronic myelomonocytic leukemia. *Leukemia*. 2008;22(7):1335-1342.

7. Aoki Y, Niihori T, Narumi Y, Kure S, Matsubara Y. The RAS/MAPK syndromes: novel roles of the RAS pathway in human genetic disorders. *Hum Mutat*. 2008;29(8):992-1006.

8. Kitahara M, Koike K, Kurokawa Y, et al. Lupus nephritis in juvenile myelomonocytic leukemia. *Clin Nephrol*. 1999;51(5):314-318.

9. Oliver JW, Farnsworth B, Tonk VS. Juvenile myelomonocytic leukemia in a child with Crohn disease. *Cancer Genet Cytogenet*. 2006;167(1):70-73.

10. Saif MW, Hopkins JL, Gore SD. Autoimmune phenomena in patients with myelodysplastic syndromes and chronic myelomonocytic leukemia. *Leuk Lymphoma*. 2002;43(11):2083-2092.

11. Flotho C, Kratz CP, Bergstrasser E, et al. Genotype-phenotype

correlation in cases of juvenile myelomonocytic leukemia with clonal RAS mutations. *Blood*. 2008;111(2):966-967.

12. Matsuda K, Shimada A, Yoshida N, et al. Spontaneous improvement of hematologic abnormalities in patients having juvenile myelomonocytic leukemia with specific RAS mutations. *Blood*. 2007;109(12):5477-5480.

13. Flotho C, Valcamonica S, Mach-Pascual S, et al. RAS mutations and clonality analysis in children with juvenile myelomonocytic leukemia (JMML). *Leukemia*. 1999;13(1):32-37.

14. Matsuda K, Sakashita K, Taira C, et al. Quantitative assessment of PTPN11 or RAS mutations at the neonatal period and during the clinical course in patients with juvenile myelomonocytic leukaemia. *Br J Haematol*. 2010;148(4):593-599.

15. Imamura M, Imai C, Takachi T, Nemoto T, Tanaka A, Uchiyama M. Juvenile myelomonocytic leukemia with less aggressive clinical course and KRAS mutation. *Pediatr Blood Cancer*. 2008;51(4):569.

16. Zhang J, Wang J, Liu Y, et al. Oncogenic Kras-induced leukemogeneis: hematopoietic stem cells as the initial target and lineage-specific progenitors as the potential targets for final leukemic transformation. *Blood*. 2009;113(6):1304-1314.

17. Sabnis AJ, Cheung LS, Dail M, et al. Oncogenic Kras initiates leukemia in hematopoietic stem cells. *PLoS Biol*. 2009;7(3):0537-0548.

18. Teachey DT, Manno CS, Axsom KM, et al. Unmasking Evans syndrome: T-cell phenotype and apoptotic response reveal autoimmune lymphoproliferative syndrome (ALPS). *Blood*. 2005;105(6):2443-2448.

19. Seif AE, Manno CS, Sheen C, Grupp SA, Teachey DT. Identifying autoimmune lymphoproliferative syndrome in children with Evans syndrome: a multi-institutional study. *Blood*. 2010;115(11):2142-2145.

Figure Legends

Figure 1

a. Flow cytometric analysis of DNT cells. CD8 and CD4 double staining was performed in TCRαβ-expressing cells.

b. Electropherogram showing KRAS G13D mutation in BM-MNC in case 1 (left panel) and case 2 (right panel).

c. Gene dosage of mutated allele in granulocyte (Gr), T cell (T) and B cell (B). Relative gene dosage was estimated by a mutant allele specific PCR method in case 1 and 2 using albumin gene as internal control.

d. Apoptosis assay using activated T cells. Apoptosis percent was measured by flow cytometry with Annexin V staining 24 and 48 hr after IL-2 depletion

e. Apoptosis percent was measured 24hr after addition of anti-FAS CH11 antibody (final 100ng/ml)

f. Western blotting analysis of Bim expression.

Figure 1

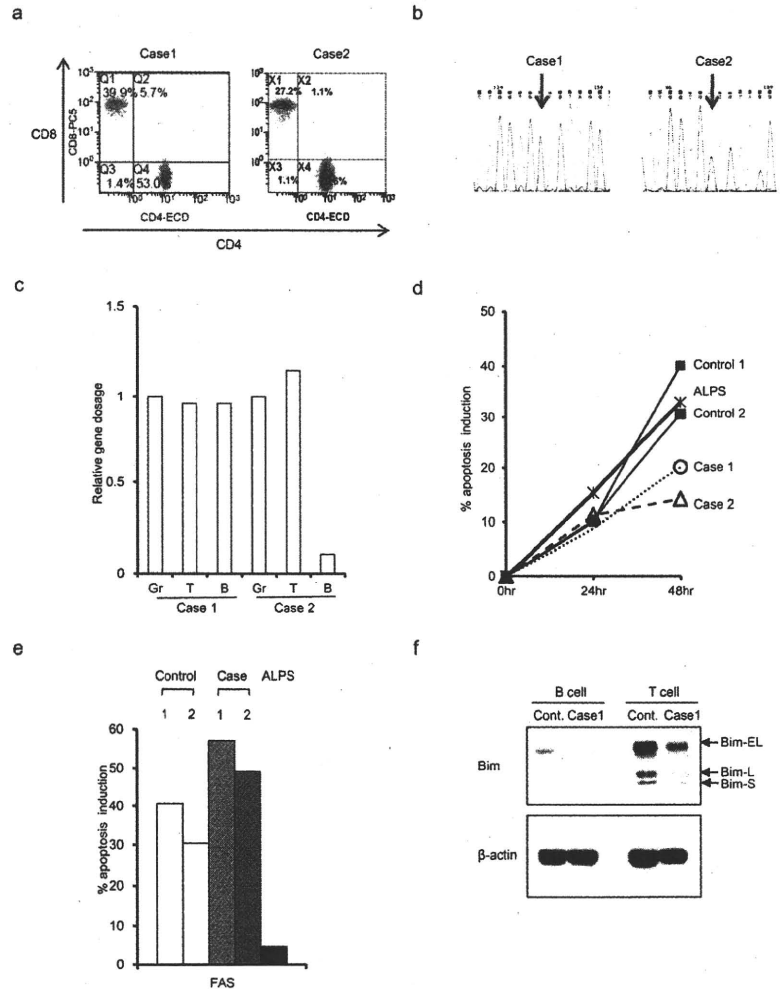
a
Case1
Case2
CD8
CD8-PC5
Q1
Q2
39.9%
5.7%
Q3
Q4
1.4%
53.0%
X1
X2
27.2%
1.1%
X3
X4
1.1%
CD4-ECD
CD4-ECD
CD4
b
Case1
Case2
c
Relative gene dosage
1.5
1
0.5
0
Gr
T
B
Gr
T
B
Case 1
Case 2
d
% apoptosis induction
50
40
30
20
10
0
Control 1
ALPS
Control 2
Case 1
Case 2
0hr
24hr
48hr
e
Control
Case
ALPS
1
2
1
2
% apoptosis induction
60
50
40
30
20
10
0
FAS
f
B cell
T cell
Cont.
Case1
Cont.
Case1
Bim
Bim-EL
Bim-L
Bim-S
β-actin

Notch2 signaling is required for proper mast cell distribution and mucosal immunity in the intestine

Mamiko Sakata-Yanagimoto,[1,2] Toru Sakai,[3] Yasuyuki Miyake,[1] Toshiki I. Saito,[2,4] Haruhiko Maruyama,[5] Yasuyuki Morishita,[6] Etsuko Nakagami-Yamaguchi,[2] Keiki Kumano,[2,7] Hideo Yagita,[8] Masashi Fukayama,[9] Seishi Ogawa,[9,10] Mineo Kurokawa,[7] Koji Yasutomo,[3] and Shigeru Chiba[1,2]

[1]Department of Clinical and Experimental Hematology, University of Tsukuba, Tsukuba, Japan; [2]Department of Cell Therapy and Transplantation Medicine, University of Tokyo Hospital, Tokyo, Japan; [3]Department of Immunology and Parasitology, Institute of Health Biosciences, The University of Tokushima Graduate School, Tokushima, Japan; [4]Laboratory of Cell Therapy, Department of Regenerative Medicine, Clinical Research Center, National Hospital Organization Nagoya Medical Center, Nagoya, Japan; [5]Parasitic Diseases Unit, Department of Infectious Diseases, Faculty of Medicine, University of Miyazaki, Miyazaki, Japan; [6]Department of Pathology, University of Tokyo, Tokyo, Japan; [7]Department of Hematology and Oncology, University of Tokyo, Tokyo, Japan; [8]Department of Immunology, Juntendo University School of Medicine, Tokyo, Japan; [9]Cancer Genomics Project, Graduate School of Medicine, University of Tokyo, Tokyo, Japan; and [10]Core Research for Evolutional Science and Technology, Japan Science and Technology Agency, Tokyo, Japan

Notch receptor-mediated signaling is involved in the developmental process and functional modulation of lymphocytes, as well as in mast cell differentiation. Here, we investigated whether Notch signaling is required for antipathogen host defense regulated by mast cells. Mast cells were rarely found in the small intestine of wild-type C57BL/6 mice but accumulated abnormally in the lamina propria of the small-intestinal mucosa of the *Notch2*-conditional knockout mice in naive status. When transplanted into mast cell–deficient W^{sh}/W^{sh} mice, *Notch2*-null bone marrow-derived mast cells were rarely found within the epithelial layer but abnormally localized to the lamina propria, whereas control bone marrow-derived mast cells were mainly found within the epithelial layer. After the infection of *Notch2* knockout and control mice with L3 larvae of *Strongyloides venezuelensis*, the abundant number of mast cells was rapidly mobilized to the epithelial layer in the control mice. In contrast, mast cells were massively accumulated in the lamina propria of the small intestinal mucosa in *Notch2*-conditional knockout mice, accompanied by impaired eradication of *Strongyloides venezuelensis*. These findings indicate that cell-autonomous Notch2 signaling in mast cells is required for proper localization of intestinal mast cells and further imply a critical role of Notch signaling in the host-pathogen interface in the small intestine. (*Blood*. 2011;117(1):128-134)

Introduction

Mast cells are important in a wide variety of physiologic and pathologic processes, including protective immune responses to parasites and allergic disorders.[1,2] In intestinal parasite infection, mast cells play a central role in the immune response.[3] During the induction phase of parasite-induced inflammation, mast cells move from the submucosa to the tip of the villi, accompanying the serial changes in the protease expression pattern. Initially, they are positive for mouse mast cell protease-5 (mMCP-5) but negative for mMCP-1 and mMCP-2; eventually, they become positive for mMCP-1 and mMCP-2 but negative for mMCP-5, demonstrating convergence from connective tissue–type mast cells (CTMCs) to mature mucosal-type mast cells (MTMCs).[4] The parasite-infected mice consequently experience jejunal mast cell hyperplasia,[5] and the serum concentration of mMCP-1, an activation marker of small intestinal mast cells, is increased by > 1000-fold compared with that in the naive status.[5]

In the mammalian immune system, we and other groups have demonstrated that Notch signaling is involved in the commitment and differentiation of T cells, the development of splenic marginal zone B cells, and the differentiation and functional modulation of mature T cells, including T-helper type I (Th1)/Th2 polarization[6,7] and differentiation of CD8-positive cytotoxic T cells.[8] Regarding the Notch signaling in mast cells, bone marrow-derived mast cells (BMMCs) highly express Jagged1[9] and Notch2[10] among the Notch ligands and the receptors, respectively. We have previously shown that signaling through the Notch2 receptor induces mast cell development from myeloid progenitors by transcriptional up-regulation of hairy and enhancer of split homolog-1 (Hes-1) and transacting T cell–specific transcription factor GATA-3 (GATA3).[11] Induction of antigen-presenting potential of mast cells by Notch signaling is also demonstrated.[12] A question yet to be solved is how Notch signaling affects mast cell properties in vivo.

In this report, we examined the effect of Notch2 signaling in in vivo mast cells using *Notch2*-conditional knockout mice.[13] We show that Notch2 signaling is specifically required for intraepithelial localization of intestinal mast cells and antiparasite immunity. In contrast, Notch2 is dispensable for either distribution or development of CTMCs.

Submitted July 9, 2010; accepted September 28, 2010. Prepublished online as *Blood* First Edition paper, October 22, 2010; DOI 10.1182/blood-2010-07-289611.

The online version of this article contains a data supplement.

The publication costs of this article were defrayed in part by page charge payment. Therefore, and solely to indicate this fact, this article is hereby marked "advertisement" in accordance with 18 USC section 1734.

Methods

Mice

The generation of *Notch2*$^{flox/flox}$ mice was described previously.[13] Mx-*Cre* transgenic mice[14] were crossed with *Notch2*$^{flox/flox}$ mice (*N2*-MxcKO mice) and the progeny were injected with polyinosinic-polycytidylic acid (pIpC; Sigma-Aldrich) 7 times every other day from 3 days after birth (25 μg/g body weight) or 3 times between 4 and 6 weeks of age (20 μg/g body weight). *N2*-MxcKO mice were further crossed with C57BL/6-Ly5.1 mice (a kind gift from Dr H. Nakauchi, University of Tokyo) to generate Ly5.1-*N2*-MxcKO mice. *Notch2* deletion in bone marrow was examined by polymerase chain reaction and 3% agarose gel electrophoresis[13] (supplemental Figure 1, available on the *Blood* Web site; see the Supplemental Materials link at the top of the online article). *W*^{sh}/*W*^{sh} mice were purchased from The Jackson Laboratory. All experiments were done with approval from the University of Tsukuba Institutional Review Board.

Staining

Sections, fixed with Carnoid fluid, were stained with 0.5% toluidine blue (Sigma-Aldrich), pH 0.3, followed by eosin. Small intestine was embedded in optimal cutting temperature (OCT) compound (TissueTek) and cut with cryostat (Leica CM1850). The section was fixed with 4% paraformaldehyde, washed with phosphate-buffered saline (PBS), blocked in 10% horse serum and 0.1% Triton-PBS, and then stained with either 1:100 goat anti-Jagged1 antibody (C-20; Santa Cruz Biotechnology), goat anti-Delta1 antibody (Genzyme Tech), or control goat immunoglobulin G (IgG; Santa Cruz Biotechnology) overnight at 4°C. The sections were washed with PBS and stained with anti–goat Alexa 594 (Invitrogen). Sections were analyzed by fluorescence microscope (Zeiss; Axioplan2), original magnification ×200.

BMMCs

Bone marrow cells from each mouse strain were cultured in RPMI 1640 medium (Sigma-Aldrich) supplemented with 10% fetal bovine serum (FBS), 50 ng/mL stem cell factor (SCF; PeproTech), and 10 ng/mL interleukin-3 (IL-3; PeproTech) for 4 weeks. Generation of BMMCs was confirmed by staining with lineage markers, c-Kit and IgE, as previously described.[11] Briefly, the cells were incubated with purified IgE (BD Biosciences) after blocking the Fcγ receptors with purified anti-CD16/32 antibody (BD Biosciences), stained with anti-IgE–fluorescein isothiocyanate (FITC; BD Biosciences), anti–Gr-1–phycoerythrin (PE), anti-Mac1–PE (eBioscience), and anti–c-Kit–allophycocyanin (APC; eBioscience), and then analyzed by FACSCalibur (BD Biosciences).

Peritoneal mast cells

Five milliliters ice-cold PBS was injected into the peritoneal cavity, and then 3 mL PBS was recovered. c-Kit and IgE receptor (FcεRI) expression was used to define the cells as peritoneal mast cells. Ly5.1 and Notch2 were stained with anti-Ly5.1–PE (BD Biosciences) or biotinylated anti-Notch2 antibody (clone HMN2-35)[8] followed by streptavidin PE (eBioscience), respectively.

Bone marrow transplantation

C57BL/6 mice and *W*^{sh}/*W*^{sh} mice were lethally irradiated with a total dose of 9.5 Gy and then transplanted with 1×10^7 whole bone marrow cells from either *N2*-MxcKO-Ly5.1 mice or *Notch2*$^{flox/flox}$-Ly5.1 mice from the tail vein. Tissues of transplanted mice were assessed at 3 to 4 months after transplantation. Donor-cell engraftment was assessed by fluorescence-activated cell sorting (FACS) analysis of peripheral blood, which was stained by anti-Ly5.2–FITC (BD Biosciences) and anti-Ly5.1–PE.

S venezuelensis infection

Mice were infected by subcutaneous injection of third-stage infective larvae of *Strongyloides venezuelensis*. The degree of infection was monitored by counting the number of eggs per gram of feces. Mast cells were counted and presented as the number per 10 villus crypt units. BMMCs were washed with PBS twice and then cultured with 10 ng/mL IL-4 and 10 ng/mL IL-10 for 3 days. These Th2-conditioned BMMCs were injected at day 3 and day 6 of experiments.[15] In contrast to the bone marrow transplantation, mice were not irradiated before BMMC injection.

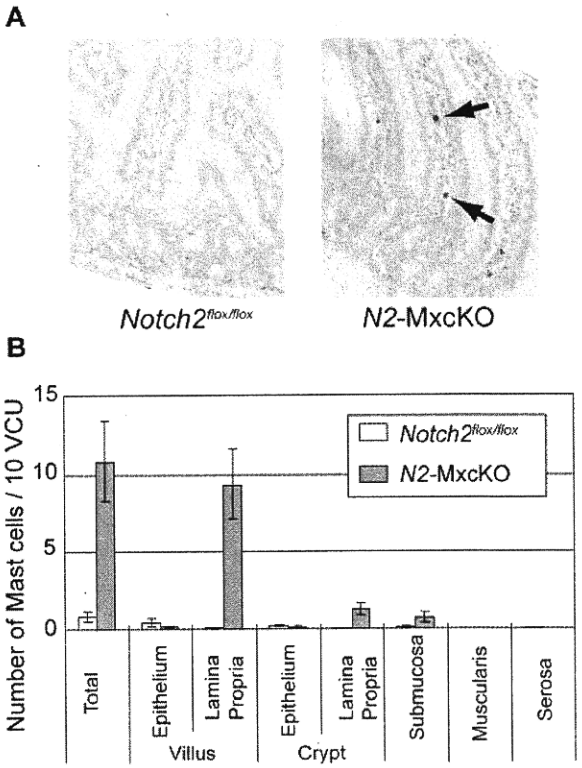

Figure 1. Mature mast cells were abnormally accumulated in the lamina propria of the small intestine of *Notch2*-deficient mice. (A) Sections of the small intestine of *N2*-MxcKO or littermate control *Notch2*$^{flox/flox}$ mice. Toluidine blue staining, followed by eosin. Original magnification ×200. (B) The numbers of mast cells per 10 villus crypt units (vcus) distributing to various layers of the small intestine. Data are presented as means ± SEM; *Notch2*$^{flox/flox}$ (n = 10) versus *N2*-MxcKO (n = 8); $P = .000461$ (total), $P = .000261$ (villus, lamina propria), $P = .001918$ (crypt, lamina propria), $P = .046874$ (submucosa).

Statistical analysis

The data for the number of mast cells and the *S venezuelensis* infection data were analyzed by the *t* test. *P* values < .05 were considered significant.

Results

Notch signaling affects the number and localization of mast cells in the small intestine

We have previously reported that Notch2 regulates mast cell differentiation in vitro.[11] To examine whether Notch2 controls the differentiation or development of MTMCs in vivo, we examined intestinal mast cells by toluidine blue staining in C57BL/6 mice carrying the *Notch2*$^{flox/flox}$ allele with or without the Mx1-*Cre* transgene (*N2*-MxcKO mice or *Notch2*$^{flox/flox}$ mice, respectively) after pIpC treatment.[13] Mast cells were only sparsely detected in the small intestine of *Notch2*$^{flox/flox}$ mice, mainly within the epithelium. However, the total number of mast cells in the small intestine of *N2*-MxcKO mice was unanticipatedly greater than that of *Notch2*$^{flox/flox}$ mice. Furthermore, those mast cells were mainly

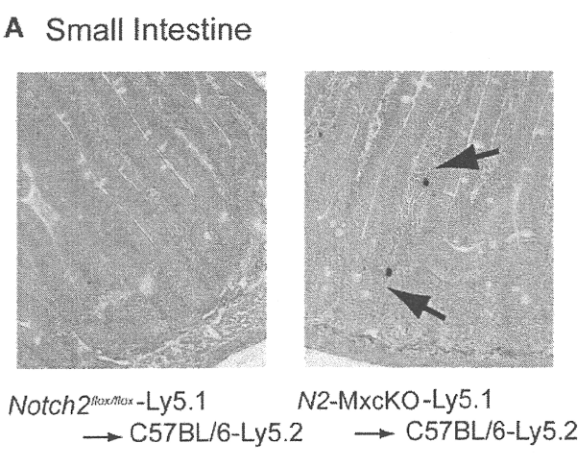

Figure 2. Localization of intestinal mast cells is abnormal in wild-type mice transplanted with *N2*-MxcKO-Ly5.1 bone marrow cells, reminiscent of that in *N2*-MxcKO mice. (A) Bone marrow cells from either *N2*-MxcKO- Ly5.1 mice or littermate *Notch2*$^{flox/flox}$- Ly5.1 mice were transplanted into lethally irradiated (9.5 Gy) C57BL/6-Ly5.2 mice. Toluidine blue staining, followed by eosin. Original magnification ×200. (B) The numbers of mast cells per 10 vcus distributing to various layers of the small intestine. Data are presented as means ± SEM; Mast cells in C57BL/6-Ly5.2 mice transplanted with *Notch2*$^{flox/flox}$-Ly5.1 (n = 3) versus *N2*-MxcKO-Ly5.1 (n = 3). P = .020594 (total) and P = .030123 (villus, lamina propria).

localized to the lamina propria, and very few mast cells were found within the epithelium (Figure 1A-B).

Localization of MTMCs is abnormal in wild-type mice transplanted with *N2*-MxcKO bone marrow cells, reminiscent of that in *N2*-MxcKO mice

Because the Mx-*Cre*–based conditional knockout system deletes target genes not only in the bone marrow cells but also, albeit partially, in the intestinal cells,[14] there was a possibility that *Notch2* deletion in the intestinal cells was responsible for the distinct distribution pattern or increased number of mast cells in *N2*-MxcKO mice compared with control mice. To exclude this possibility, we transplanted *Notch2*-null bone marrow cells carrying the Ly5.1 marker to irradiated wild-type C57BL/6-Ly5.2 mice. A chimerism of donor-derived Ly5.1-positive fraction accounted for more than 70% in the peripheral blood (data not shown). The recipients of bone marrow cells from *Notch2*$^{flox/flox}$ mice showed that the intestinal mast cell distribution was virtually the same as that in wild-type mice, whereas the recipients of *Notch2*-null bone marrow cells showed an increase in mast cells mainly in the lamina propria in an indistinguishable manner from the *N2*-MxcKO mice (Figure 2A-B). This result indicates that deletion of *Notch2* in bone marrow-derived cells alters the distribution pattern and increases the number of mast cells in the small intestine.

Notch-ligand expression in the small intestine

Notch signaling is known to be activated through Notch ligand-receptor binding.[16] We examined the expression pattern of Notch ligands in the small intestine with antibodies against Notch ligands Jagged1 and Delta1 and found that the epithelial layer was clearly stained with anti-Jagged1 but not with anti-Delta1 antibody (Figure 3). The staining with the anti-Jagged1 antibody was confined to the surface of epithelial cells, especially at their basal side rather than the apical side (Figure 3). The Jagged1 expression pattern suggests a possibility that Jagged1-Notch2 interaction between the basal side of the epithelial cells and mast cells has an important role for mast cell migration from the lamina propria across the basement membrane toward the epithelium (Figure 3). Furthermore, the ligand-receptor binding itself might contribute to mast cell–epithelial cell adhesion to some extent, based on our observation that *Notch2*-expressing BMMCs attached to the Jagged1-expressing Chinese hamster ovary (CHO) cells, while *Notch2*-null BMMCs did not (supplemental Figure 2).

Notch2 is dispensable for the CTMC development and distribution

We next investigated the roles of Notch2 in the development of CTMCs. The localization and the number of CTMCs in the skin and peritoneal cavity were not significantly different between *N2*-MxcKO and littermate *Notch2*$^{flox/flox}$ mice more than 4 weeks after the treatment with pIpC (data not shown). This observation might simply indicate that the Mx-*Cre* system was inefficient in the tissue-resident mast cells, as a great majority of peritoneal

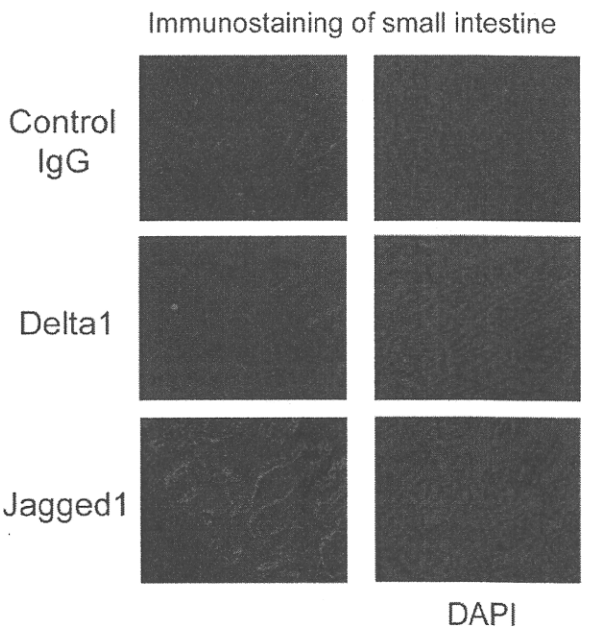

Figure 3. Jagged1 is strongly expressed on the surface of the epithelial cells, especially at their basal side. A section of small intestine prepared using cryostat was stained with goat anti-Jagged1 and goat anti-Delta1 antibodies followed by anti–goat Alexa594. Original magnification ×200.

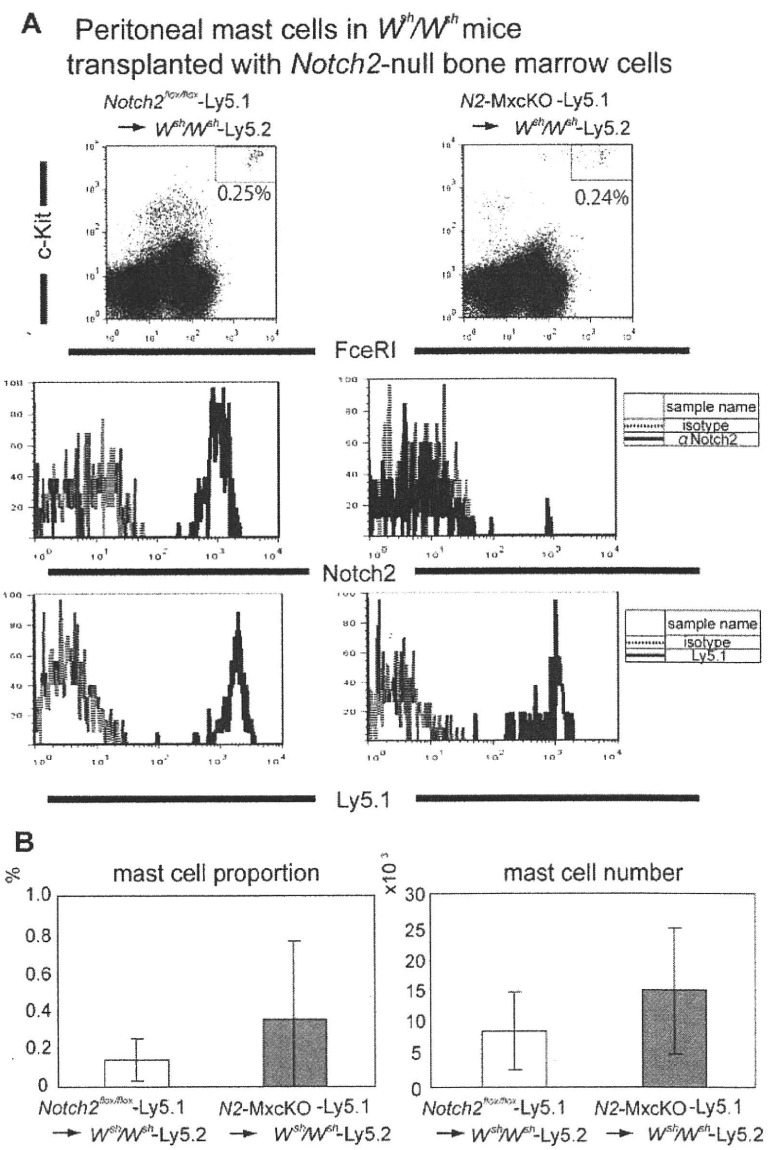

Figure 4. Notch2 is not required for peritoneal mast cell development. (A) Bone marrow cells from *N2*-MxcKO-Ly5.1 mice or control *Notch2*$^{flox/flox}$-Ly5.1 mice were transplanted into lethally irradiated W^{sh}/W^{sh} mice. Peritoneal mast cells were stained with anti–c-Kit–APC, IgE, and biotinylated anti-Notch2 antibody (HMN2-35), followed by anti-IgE–FITC and streptavidin-PE, or they were stained with anti–c-Kit–APC, IgE, and anti-Ly 5.1–PE, followed by anti-IgE–FITC; they were then analyzed by FACSCalibur (BD Biosciences). (B) The proportion (left) and the absolute number (right) of peritoneal mast cells were not significantly different between W^{sh}/W^{sh} mice transplanted with *Notch2*-WT bone marrow cells and those transplanted with *Notch2*-null bone marrow cells. $P = .210642$ (mast cell proportion) and $P = .196045$ (mast cell number).

mast cells of pIpC-treated *N2*-MxcKO mice still expressed Notch2 (data not shown). Therefore, to clarify the requirement of *Notch2* in the CTMC development, we examined peritoneal mast cells in mast cell-deficient W^{sh}/W^{sh} mice after transplantion of *Notch2*-null bone marrow cells carrying the Ly5.1 marker. In this system, mast cells exclusively develop from transplanted bone marrow progenitors, in which the *Cre* recombinase under the Mx-promoter is quite effective [14] (supplemental Figure 1). In this experiment, we found that the proportion and absolute number of peritoneal mast cells was not significantly different between those developed from the *N2*-MxcKO-Ly5.1 bone marrow cells and those developed from littermate *Notch2*$^{flox/flox}$-Ly5.1 bone marrow cells (Figure 4A-B). Notch2 was not expressed in the peritoneal mast cells derived from *N2*-MxcKO-Ly5.1 bone marrow cells but was expressed in those derived from littermate *Notch2*$^{flox/flox}$-Ly5.1 bone marrow cells (Figure 4A middle), indicating that *Notch2* was deleted efficiently. These results suggest that Notch2 is dispensable for the development and distribution of CTMCs.

Cell-autonomous Notch2 signaling in mast cells is important for mast cell migration across the basement membrane in the small intestine

We then asked a question whether aberrant mast cell migration in the small intestine in *N2*-MxcKO mice is dependent on Notch2 signaling in mast cells per se. We intravenously infused *Notch2*-null or control BMMCs into nonirradiated W^{sh}/W^{sh} mice after *S venezuelensis* infection, because it is reported that BMMCs could only transiently reconstitute intestinal mast cells in mast-cell deficient mice if these recipient mice are in naive status.[17] In tissue sections, we found that the distribution of mast cells in the small intestine was different between control BMMCs-reconstituted mice and *Notch2*-null BMMCs-reconstituted mice; control BMMCs were mainly migrated into the epithelial layer, while a majority of *Notch2*-null BMMCs remained in the lamina propria. This observation indicates that mast cell-autonomous Notch2 expression contributes to mast cell migration across the basement membrane from lamina propria into the epithelial layer (Figure 5A-B). Even in the control BMMC-infused mice, however, a substantial proportion of

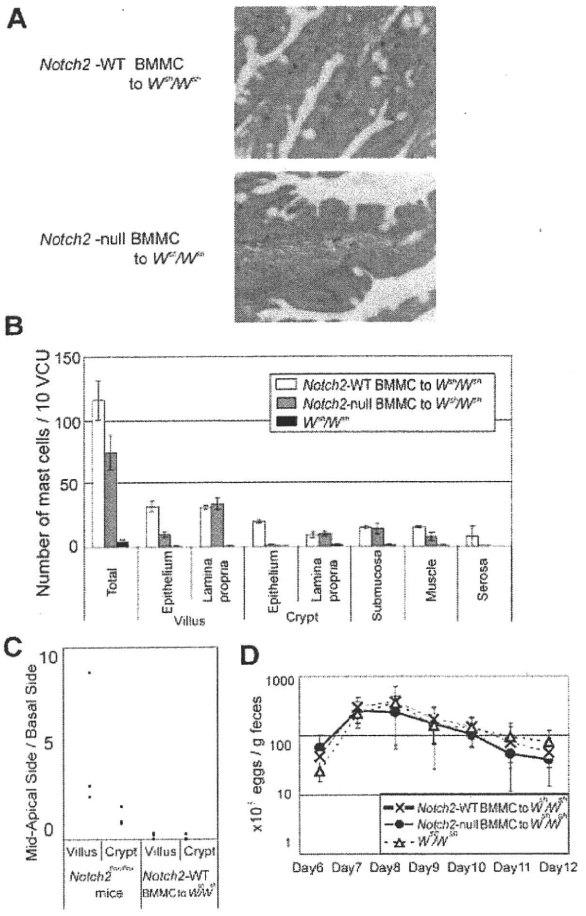

Figure 5. Mast cell–autonomous Notch2 expression is required for mast cell migration toward the epithelium. W^{sh}/W^{sh} mice infected with *S venezuelensis* were intravenously infused with Th2-conditioned *Notch2*-null or control BMMCs on days 3 and 6 of infection. (A) *Notch2*-null BMMCs poorly migrated toward the epithelium compared with control BMMCs. Toluidine blue staining followed by eosin staining. Original magnification ×200. (Top) Control BMMCs; (Bottom) *Notch2*-null BMMCs. (B) The number of mast cells per 10 vcus in the small intestine on day 12 after *S venezuelensis* infection in W^{sh}/W^{sh} mice, without BMMC infusion, with control BMMC infusion, and with *Notch2*-null BMMC infusion. Data are presented as means ± SEM; n = 3 (control BMMC infusion) and n = 4 (*Notch2*-null BMMC infusion). $P = .004080$ (villus, epithelium) and $P = .000020$ (crypt, epithelium). Note that mast cells in W^{sh}/W^{sh} mice infused with *Notch2*-null BMMCs abnormally resided in the lamina propria, whereas most of those in W^{sh}/W^{sh} mice infused with control BMMCs had intraepithelially migrated. (C) Mast cell number in mid to apical side of the epithelial layer was divided with that in the basal side of the epithelial layer. (D) Time course of *S venezuelensis* egg numbers in the stool. The number of excreted eggs was not significantly different between W^{sh}/W^{sh} mice infused with *Notch2*-null and control BMMCs. Data are presented as means ± SEM.

mast cells still remained in the lamina propria, submucosa, and smooth muscle layers, and the distribution of mast cells within the epithelium was confined to the basement membrane side of the epithelial layer (Figure 5B-C). This mast cell localization pattern was different from that in the $Notch2^{flox/flox}$ mice with *S venezuelensis* infection, in which mast cells were present mainly at the mid to apical side of the epithelial layer (Figure 5C). The numbers of *S venezuelensis* eggs in the stool were virtually the same in the *S venezuelensis*–infected W^{sh}/W^{sh} mice infused with *Notch2*-null and control BMMCs and in the *S venezuelensis*–infected W^{sh}/W^{sh} mice without any BMMC infusion throughout the period after infection (Figure 5D).

Taken together, the BMMC-W^{sh}/W^{sh} transplantation model demonstrated that Notch2 in the mast cells indeed determines their intraepithelial migration from lamina propria; nevertheless, this model was not adequate to examine the physiologic mast cell distribution pattern and subsequent parasite expulsion that depends on mast cells.

Notch2 signaling regulates antiparasite immunity of mast cells in the intestine

The BMMC-W^{sh}/W^{sh} reconstitution model could not completely reflect physiologic mast cell distribution pattern in the small intestine. Therefore, to further assess the effect of Notch2 signaling on the mucosal immune response of intestinal mast cells under a pathologic condition, *N2*-MxcKO or control $Notch2^{flox/flox}$ mice were infected with *S venezuelensis*. Total mast cell number was increased in $Notch2^{flox/flox}$ mice much more than in *N2*-MxcKO mice, especially in the epithelium in both crypts and villi 8 days after infection (Figure 6A-B). Thirteen days after infection, mast cells in the epithelium in $Notch2^{flox/flox}$ mice were still more abundant than those in *N2*-MxcKO mice (Figure 6C-D), while mast cell accumulation in the lamina propria in *N2*-MxcKO mice was more prominent in both villi and crypt than that in the earlier stage of infection (Figure 6A,C). In particular, dense aggregation of mast cells was prominent in the lamina propria of *N2*-MxcKO mice at the tip of the villi (Figure 6D). As a consequence, the total number of mast cells in the intestine of *N2*-MxcKO mice became equivalent to those of $Notch2^{flox/flox}$ mice 13 days after infection (Figure 6C,E). The number of *S venezuelensis* eggs in the stool was gradually decreased during day 8 to 10 in control $Notch2^{flox/flox}$ mice but not in *N2*-MxcKO mice (Figure 6F). Furthermore, the worms were still observed in *N2*-MxcKO mice but not in $Notch2^{flox/flox}$ mice 12 days after infection (Figure 6G). These data suggest that Notch2 deficiency alters the distinct distribution pattern of mast cells in the small intestine, which is responsible for the defective eradication of *S venezuelensis*.

Discussion

There is a growing body of evidence that Notch signaling modulates cellular migration and adhesion in endothelial, neural, and lymphoid lineage cells, as well as cancer cells.[18] We have shown that Notch2 signaling induces the development of mast cells.[11] However, it has remained unclear whether Notch2 signaling is involved in the distribution of mast cells in the intestinal mucosa or connective tissues or in controlling the functions of mast cells against microorganisms. Here, we investigated the role of Notch2 signaling in mast cells in terms of their distribution and functions using cell-specific *Notch2*-deficient mice. We found that in *N2*-MxcKO mice, mast cells were abnormally accumulated in the lamina propria of the small intestine, suggesting that *Notch2*-null mast cells have some defect in the migration toward the epithelium. Furthermore, *N2*-MxcKO mice failed to eradicate *S venezuelensis* and exhibited a distinct mast cell migration pattern in the intestine compared with control mice, suggesting that mast cells regulate the host-microbial interface in the intestine through Notch2 signaling.

Mast cell number was rather increased in the intestinal mucosa of *N2*-MxcKO mice compared with control mice in naive status. Mast cell progenitors were supposed to reside in the submucosa and gradually move toward the villi, accompanied by their differentiation into mature mast cells. Based on our observation in

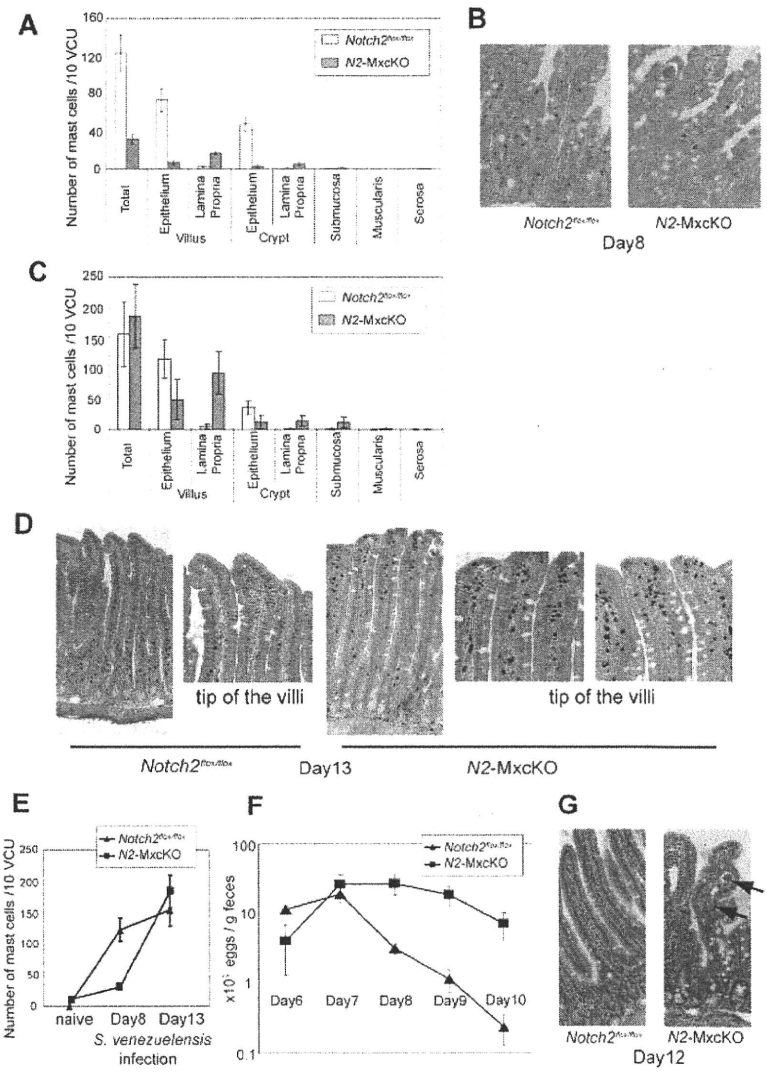

Figure 6. Notch2 is essential for antiparasite immunity of mast cells in the intestine. *N2*-MxcKO or control *Notch2*$^{flox/flox}$ mice were subcutaneously injected with third-stage infective larvae of *S venezuelensis*. (A) The number of mast cells per 10 vcus in the small intestine on day 8 after *S venezuelensis* infection. Data are presented as means ± SEM. The number of mast cells was much less in *N2*-MxcKO mice; n = 3, $P = .008592$ (total), $P = .005695$ (villus, epithelium), $P = .000715$ (villus, lamina propria), $P = .005245$ (crypt, epithelium), and $P = .045466$ (crypt, lamina propria). Note that mast cells in *N2*-MxcKO mice were abnormally clustered in the lamina propria, whereas most of those in the control *Notch2*$^{flox/flox}$ mice were intraepithelially migrated. (B) Toluidine blue staining followed by eosin staining of the small intestine on day 8; original magnification ×200. (C) The number of mast cells per 10 vcus in the small intestine on day 13 after *S venezuelensis* infection. Data are presented as means ± SEM; n = 3, $P = .026076$ (villus, epithelium), $P = .00194$ (villus, lamina propria), $P = .021177$ (crypt, epithelium), and $P = .019324$ (crypt, lamina propria), $P = .047445$ (submucosa). (D) Toluidine blue staining followed by eosin staining of the small intestine on day 13. Original magnification ×200. (E) The total number of mast cells per 10 vcus on day 0, day 8, and day 13 of infection. The total number of mast cells was significantly lower in *N2*-MxcKO mice at the early phase (day 8) and almost equal at the later phase (day 13) to that of control mice. Data are presented as means ± SEM; n = 10 and 8 (day 0, *Notch2*$^{flox/flox}$ and *N2*-MxcKO); n = 3 and 3 (day 8, *Notch2*$^{flox/flox}$ and *N2*-MxcKO); n = 4 and 4 (day 13, *Notch2*$^{flox/flox}$ and *N2*-MxcKO). (F) Time course of egg number in the stool. The number of excreted eggs was significantly greater in *N2*-MxcKO mice compared with those in *Notch2*$^{flox/flox}$ mice. Data are represented as means ± SEM; n = 4; $P = .0291$ (day 8) and $P = .0219$ (day 9). (G) Hematoxylin-eosin staining of the small intestine on day 12. Original magnification ×200. Arrows indicate worms. Worms were still observed in the villi in the jejunum of *N2*-MxcKO, but not of *Notch2*$^{flox/flox}$ mice.

an *S venezuelensis*–infection model, mast cells increase in number in the epithelium in control *Notch2*$^{flox/flox}$ mice, while they abnormally aggregate in lamina propria in *N2*-MxcKO mice, especially in the later stage of infection. This suggests that mast cell migration from lamina propria toward the epithelium across the basement membrane is impaired in *N2*-MxcKO mice. Consequently, mast cell turnover might be prolonged in *N2*-MxcKO mice. Given that the mechanism of mast cell migration from lamina propria toward the epithelium is common in naive status and infection status, such migration defect may also explain the mast cell increase in *N2*-MxcKO mice in naive status that we observed.

The defect of mast cell migration toward intraepithelium of the small intestine in *N2*-MxcKO mice is very similar to that in integrin β6-deficient mice,[19] in which activation of transforming growth factor (TGF)–β signaling is impaired.[20] A crosstalk between Notch signaling and TGF-β signaling might occur in intestinal mast cells as well as the cases of other cell types.[21] Alternatively, Notch signaling might directly regulate a downstream target of TGF-β1 in intestinal mast cell migration (eg, the induction of integrin αE expression).[19,22] Integrin αE, forming an integrin αEβ7 complex on mast cells, binds to E-cadherin on epithelial cells and is involved in mast cell localization in the epithelium.[22] The expression level of integrin αEβ7, measured by flow cytometric analysis, however, was not affected by Notch-ligand stimulation in BMMCs (unpublished data).

In the previous paper we showed that Notch signaling facilitates mast cell lineage development at the expense of granulocyte/macrophage development from both common myeloid progenitors (CMPs) and granulocyte-macrophage progenitors (GMPs) in vitro.[11] Mast cells, however, were not depleted in *N2*-MxcKO mice in naive status in vivo, but rather slightly increased in the small intestine of *N2*-MxcKO mice. This clearly indicates that Notch2 signaling is dispensable for steady-state mast cell generation in vivo. However, the dynamic increase of mast cells during the early phase of intestinal parasite infection was markedly impaired in *N2*-MxcKO mice. The mechanisms underlying the Notch2 signaling requirement only in parasite-infected mice remain to be clarified. Nevertheless, rapidly increasing intestinal mast cells have to be supplied by mast cell progenitors. The pathways and mechanisms responsible for mast cell progenitor recruitment and trafficking are likely to be dynamic and susceptible to modification during inflammation.[1] Such a modulation of the mast cell generation pathway during intestinal infection might underlie the requirement of *Notch2* only during parasite infection. This is similar to

IL-3–deficient mice. IL-3 is essential for mast cell differentiation in vitro; however, IL-3–deficient mice have the normal number of mast cells at the steady state, whereas mast cell hyperplasia is impaired upon intestinal parasite infection.[23]

Our data showed that parasite expulsion was impaired in *N2*-MxcKO mice. We could not exclude the possibility that the *Notch2* deletion in immune cells other than mast cells modulate the response against the nematode infection. If we could show that Th2-conditioned wild-type BMMCs successfully eradicate *S venezuelensis* in W^{sh}/W^{sh} mice and that *Notch2*-null BMMCs do not, it would be clearer that Notch2 signaling in mast cells per se but not in other immune cells should be critically important for defense against *S venezuelensis* infection. The failure of rescue experiments may be caused by the abnormal mast cell distribution pattern of wild-type BMMCs in W^{sh}/W^{sh} mice. Nevertheless, the result of this experiment supported the previous finding that the proper epithelial migration of mast cells is required for efficient expulsion of *S venezuelensis*[24] and thus provides an insight that the impaired *S venezuelensis* expulsion in *N2*-MxcKO mice is attributed to the mast cell-autonomous deletion of *Notch2*.

In conclusion, our data clearly indicate that Notch2 receptor signaling is specifically required for proper intestinal mast cell distribution in a cell-autonomous manner. Furthermore, involvement of Notch2 signaling in mucosal immunity was proven, particularly for eradication of infected parasites, although whether this is due to the Notch2 signaling in mast cells is yet to be elucidated.

Acknowledgments

We thank Dr Shigeo Koyasu for kind advice on the parasite infection experiment and Dr Cliff Takemoto, Dr Eichi Morii, and Dr Keisuke Oboki for kind advice on the histochemistry. We also thank Dr Hiromitsu Nakauchi for the Ly5.1 mice.

This work was supported in part by Grants-in-Aid for Scientific Research from the Japan Society for the Promotion of Science (KAKENHI #21790905 to M.S.-Y. and #18659276 to S.C.) and by grants from Mitsubishi Pharma Research Foundation and Takeda Science Foundation.

Authorship

Contribution: M.S.-Y. designed and performed the research, analyzed the data, and wrote the paper; T.S., Y. Miyake, and Y. Morishita performed the research; T.I.S., H.M., and H.Y. contributed new reagents; E.N.-Y., K.K., M.F., S.O., and M.K. provided vital discussion; K.Y. designed the research; and S.C. designed the research, analyzed the data, and wrote the paper.

Conflict-of-interest disclosure: The authors declare no competing financial interests.

Correspondence: Shigeru Chiba, Department of Clinical and Experimental Hematology, University of Tsukuba, 1-1-1 Tennodai, Tsukuba, Ibaraki, 305-8575, Japan; e-mail: schiba-tky@umin.net.

References

1. Gurish MF, Boyce JA. Mast cells: ontogeny, homing, and recruitment of a unique innate effector cell. *J Allergy Clin Immunol.* 2006;117(6):1285-1291.
2. Galli SJ, Nakae S, Tsai M. Mast cells in the development of adaptive immune responses. *Nat Immunol.* 2005;6(2):135-142.
3. Maruyama H, Yabu Y, Yoshida A, Nawa Y, Ohta N. A role of mast cell glycosaminoglycans for the immunological expulsion of intestinal nematode, Strongyloides venezuelensis. *J Immunol.* 2000; 164(7):3749-3754.
4. Friend DS, Ghildyal N, Gurish MF, et al. Reversible expression of tryptases and chymases in the jejunal mast cells of mice infected with Trichinella spiralis. *J Immunol.* 1998;160(11):5537-5545.
5. Miller HR, Pemberton AD. Tissue-specific expression of mast cell granule serine proteinases and their role in inflammation in the lung and gut. *Immunology.* 2002;105(4):375-390.
6. Tsukumo S, Yasutomo K. Notch governing mature T-cell differentiation. *J Immunol.* 2004; 173(12):7109-7113.
7. Radtke F, Wilson A, Mancini SJ, MacDonald HR. Notch regulation of lymphocyte development and function. *Nat Immunol.* 2004;5(3):247-253.
8. Maekawa Y, Minato Y, Ishifune C, et al. Notch2 integrates signaling by the transcription factors RBP-J and CREB1 to promote T-cell cytotoxicity. *Nat Immunol.* 2008;9(10):1140-1147.
9. Singh N, Phillips RA, Iscove NN, Egan SE. Expression of notch receptors, notch ligands, and fringe genes in hematopoiesis. *Exp Hematol.* 2000;28(5):527-534.
10. Jonsson JI, Xiang Z, Pettersson M, Lardelli M, Nilsson G. Distinct and regulated expression of Notch receptors in hematopoietic lineages and during myeloid differentiation. *Eur J Immunol.* 2001;31(11):3240-3247.
11. Sakata-Yanagimoto M, Nakagami-Yamaguchi E, Saito T, et al. Coordinated regulation of transcription factors through Notch2 is an important mediator of mast cell fate. *Proc Natl Acad Sci U S A.* 2008;105(22):7839-7844.
12. Nakano N, Nishiyama C, Yagita H, et al. Notch signaling confers antigen-presenting cell functions on mast cells. *J Allergy Clin Immunol.* 2009; 123(1):74-81 e71.
13. Saito T, Chiba S, Ichikawa M, et al. Notch2 is preferentially expressed in mature B cells and indispensable for marginal zone B lineage development. *Immunity.* 2003;18(5):675-685.
14. Kuhn R, Schwenk F, Aguet M, Rajewsky K. Inducible gene targeting in mice. *Science.* 1995; 269(5229):1427-1429.
15. Fukao T, Yamada T, Tanabe M, et al. Selective loss of gastrointestinal mast cells and impaired immunity in PI3K-deficient mice. *Nat Immunol.* 2002;3(3):295-304.
16. Kopan R, Ilagan MX. The canonical Notch signaling pathway: unfolding the activation mechanism. *Cell.* 2009;137(2):216-233.
17. Tanzola MB, Robbie-Ryan M, Gutekunst CA, Brown MA. Mast cells exert effects outside the central nervous system to influence experimental allergic encephalomyelitis disease course. *J Immunol.* 2003;171(8):4385-4391.
18. Nam DH, Jeon HM, Kim S, et al. Activation of notch signaling in a xenograft model of brain metastasis. *Clin Cancer Res.* 2008;14(13):4059-4066.
19. Brown JK, Knight PA, Pemberton AD, et al. Expression of integrin-alphaE by mucosal mast cells in the intestinal epithelium and its absence in nematode-infected mice lacking the transforming growth factor-beta1-activating integrin alphav-beta6. *Am J Pathol.* 2004;165(1):95-106.
20. Munger JS, Huang X, Kawakatsu H, et al. The integrin alpha v beta 6 binds and activates latent TGF beta 1: a mechanism for regulating pulmonary inflammation and fibrosis. *Cell.* 1999;96(3): 319-328.
21. Kluppel M, Wrana JL. Turning it up a Notch: cross-talk between TGF beta and Notch signaling. *Bioessays.* 2005;27(2):115-118.
22. Wright SH, Brown J, Knight PA, Thornton EM, Kilshaw PJ, Miller HR. Transforming growth factor-beta1 mediates coexpression of the integrin subunit alphaE and the chymase mouse mast cell protease-1 during the early differentiation of bone marrow-derived mucosal mast cell homologues. *Clin Exp Allergy.* 2002;32(2):315-324.
23. Lantz CS, Boesiger J, Song CH, et al. Role for interleukin-3 in mast-cell and basophil development and in immunity to parasites. *Nature.* 1998; 392(6671):90-93.
24. Abe T, Nawa Y. Localization of mucosal mast cells in W/Wv mice after reconstitution with bone marrow cells or cultured mast cells, and its relation to the protective capacity to Strongyloides ratti infection. *Parasite Immunol.* 1987;9(4):477-485.

T Cell Leukemia/Lymphoma 1 and Galectin-1 Regulate Survival/Cell Death Pathways in Human Naive and IgM$^+$ Memory B Cells through Altering Balances in Bcl-2 Family Proteins[1]

Siamak Jabbarzadeh Tabrizi,* Hiroaki Niiro,[2†] Mariko Masui,[‡] Goichi Yoshimoto,[†] Tadafumi Iino,[§] Yoshikane Kikushige,[†] Takahiro Wakasaki,[¶] Eishi Baba,[†] Shinji Shimoda,[†] Toshihiro Miyamoto,[‡] Toshiro Hara,* and Koichi Akashi[†§]

BCR signaling plays a critical role in purging the self-reactive repertoire, or in rendering it anergic to establish self-tolerance in the periphery. Differences in self-reactivity between human naive and IgM$^+$ memory B cells may reflect distinct mechanisms by which BCR signaling dictates their survival and death. Here we demonstrate that BCR stimulation protected naive B cells from apoptosis with induction of prosurvival Bcl-2 family proteins, Bcl-x_L and Mcl-1, whereas it rather accelerated apoptosis of IgM$^+$ memory B cells by inducing proapoptotic BH3-only protein Bim. We found that BCR-mediated PI3K activation induced the expression of Mcl-1, whereas it inhibited Bim expression in B cells. Phosphorylation of Akt, a downstream molecule of PI3K, was more sustained in naive than IgM$^+$ memory B cells. Abundant expression of T cell leukemia/lymphoma 1 (Tcl1), an Akt coactivator, was found in naive B cells, and enforced expression of Tcl1 induced a high level of Mcl-1 expression, resulting in prolonged B cell survival. In contrast, Galectin-1 (Gal-1) was abundantly expressed in IgM$^+$ memory B cells, and inhibited Akt phosphorylation, leading to Bim up-regulation. Enforced expression of Gal-1 induced accelerated apoptosis in B cells. These results suggest that a unique set of molecules, Tcl1 and Gal-1, defines distinct BCR signaling cascades, dictating survival and death of human naive and IgM$^+$ memory B cells. *The Journal of Immunology,* **2009, 182: 1490–1499.**

Primary human peripheral B cells are made up of heterogeneous subpopulations that include a high proportion of memory B cells compared with those in rodents. Due to the advantage conferred by the usefulness of CD27 as a memory marker in humans, peripheral B cells are divided into at least three distinct subsets: naive (IgM$^+$CD27$^-$), IgM$^+$ memory (IgM$^+$ CD27$^+$), and switched memory (IgG$^+$A$^+$CD27$^+$) B cells (1). Of particular interest are IgM$^+$ memory B cells in that they do not exist in mice and could develop through the novel germinal center-independent pathways and express somatically mutated IgM Abs (2). To date, IgM$^+$ memory B cells have been proposed to be circulating splenic marginal zone (MZ)[3] B cells and to play a critical role in the protection against encapsulated organisms (2, 3). Although in vivo function of IgM$^-$ memory B cells is becoming evident (4), the molecular mechanisms of activation of this subset remain poorly characterized.

Due to random rearrangements of the subunits of a functional BCR from genomic cassettes, a large proportion of developing human B cells in the bone marrow express self-reactive BCRs, but most of these potentially noxious BCRs are purged from the repertoire at several checkpoints in the bone marrow and the periphery (5). Nevertheless, up to 20% of mature naive B cells in normal peripheral blood still express low-affinity self-reactive BCRs (5). In sharp contrast, IgM$^-$ memory B cells isolated from normal donors are devoid of such self-reactive BCRs (6). These findings suggest a distinct homeostatic control of human naive and IgM$^+$ memory B cells.

BCR transmits the signals that are critical for both the elimination of self-reactive repertoire and the expansion of pathogen-specific repertoire. Upon BCR ligation by Ags, Lyn and Syk protein tyrosine kinases are initially activated. Syk propagates the signal by phosphorylating downstream signaling molecules. This results in activation of key signaling intermediates PI3K and phospholipase C (PLC)γ2. PI3K activates Akt kinase, which is critical for B cell survival (7). PLCγ2 activation leads to the release of intracellular Ca^{2-} and protein kinase C activation, which in turn cause activation of MAPK family kinases (ERK, JNK, and p38 MAPK) and transcription factors including NF-κB and NF-AT. These outputs subsequently connect with further-downstream molecules responsible for determining B cell fates such as survival, growth, and differentiation.

*Department of Pediatrics, Graduate School of Medical Sciences, Kyushu University, Fukuoka, Japan; †Department of Medicine and Biosystemic Science, Graduate School of Medical Sciences, Kyushu University, Fukuoka; ‡Center for Cellular and Molecular Medicine, Kyushu University Hospital, Fukuoka, Japan; §Department of Cancer Immunology and AIDS, Dana-Farber Cancer Institute, MA 02115; and ¶Department of Otorhinolaryngology, Graduate School of Medical Sciences, Kyushu University, Fukuoka, Japan

Received for publication August 7, 2008. Accepted for publication November 15, 2008.

The costs of publication of this article were defrayed in part by the payment of page charges. This article must therefore be hereby marked *advertisement* in accordance with 18 U.S.C. Section 1734 solely to indicate this fact.

[1] This work was supported in part by a Grant-in-Aid from the Ministry of Education, Culture, Sports, Science, and Technology in Japan (to S.J.T., H.N., T.H., and K.A.).

[2] Address correspondence and reprint requests to Dr. Hiroaki Niiro, Department of Medicine and Biosystemic Science, Graduate School of Medical Sciences, Kyushu University, 3-1-1 Maidashi, Higashi-ku, Fukuoka 812-8582, Japan. E-mail address: hniiro@med.kyushu-u.ac.jp

[3] Abbreviations used in this paper: MZ, marginal zone; Gal-1, galectin-1; Tcl1, T cell leukemia/lymphoma 1; PLC, phospholipase C; h, human; EGFP, enhanced GFP; CLL, chronic lymphocytic leukemia; BAFF, B cell-activating factor of the TNF family.

The Bcl-2-regulated pathway plays a critical role in BCR-induced survival and death (8, 9). The Bcl-2 family proteins fall into three subgroups: the first subgroup including Bcl-2, Bcl-x_L, and Mcl-1 inhibits some apoptotic pathways; the second subgroup including Bax and Bak directly induces apoptosis by promoting cytochrome *c* release from the mitochondria; the third subgroup, called BH3-only proteins, consists of at least eight mammalian proapoptotic proteins and is activated in a stimulus-specific, as well as a cell type-specific, manner. Among Bcl-2 family proteins, a BH3-only protein Bim is particularly important in controlling lymphocyte apoptosis. Bim deficiency causes a substantial expansion of autoreactive B cells leading to autoimmune diseases (10). B cells lacking Bim are refractory to BCR-induced apoptosis (10). Bim preferentially binds anti-apoptotic Mcl-1 (11, 12). Conditional knockout of Mcl-1 causes premature death of immature and mature B cells (12), suggesting a pivotal role of Mcl-1 in B cell survival. Based on these findings, tipping the balance between Mcl-1 and Bim expression may be a critical determinant for B cell survival and death. To date, little is known about how BCR signaling dictates the survival and death of human B cell subsets via the Bcl-2-regulated pathway.

In this study, we demonstrate that BCR stimulation rescued naive B cells from apoptosis with Bcl-x_L and Mcl-1 induction, whereas it rather accelerated apoptosis of IgM^+ memory B cells with Bim induction. Sustained Akt activation in naive but not IgM^+ memory B cells appears to be critical for reciprocal expression pattern of these Bcl-2 family proteins. Moreover, we demonstrate that T cell leukemia/lymphoma 1 (Tcl1) and galectin-1 (Gal-1), abundantly expressed in naive and IgM^+ memory B cells, respectively, play a crucial role in regulating Akt activation, thereby affecting their survival and death via the Bcl-2-regulated pathway.

Materials and Methods

Reagents

PE-Cy5-conjugated mouse anti-human (h) CD3, -hCD4, -hCD8, -hCD11b, -hCD14, -hCD56, and -human glycophorin A mAbs; FITC-conjugated mouse anti-hCD19, -hCD69, -hCD86, -hCD95 mAbs; and PE-conjugated mouse anti-hCD27 mAb were purchased from BD Immunocytometry. FITC-conjugated goat anti-hIgM, -hIgD, -hIgG, -hIgA, rabbit anti-hGal-1 sera and recombinant hGal-1 were obtained from MBL. Goat anti-hIgM and IgG/IgA/IgM $F(ab')_2$ fragments were purchased from Jackson ImmunoResearch Laboratories. Rabbit anti-human phospho-ZAP70/Syk, anti-human phospho-PLCγ2 (Y1217), anti-human phospho-JNK, anti-human phospho-ERK, anti-human phospho-Akt, anti-human Bim, anti-human Tcl1 sera, and rabbit anti-human phospho-p85/p70 S6K, anti-human phospho-NF-κB p65, and anti-human Bcl-x_L mAbs were from Cell Signaling Technology. Mouse anti-β-actin mAb and rabbit anti-human Mcl-1 sera were from Sigma-Aldrich. A PI3K inhibitor (Ly294002) was purchased from Calbiochem (EMD Biosciences).

Isolation and culture of B cell subsets

Human PBMCs were separated from buffy coats kindly provided by Fukuoka Red Cross Blood Center (Chikushino, Japan). The buffy coats originate from kind whole blood donations of RBC transfusion by healthy volunteers (age range, 18–55 years). Informed consent was obtained from all subjects. B cells were isolated with Dynabeads M450 CD19 and DETACHaBEAD CD19 (Dynal Biotech) according to the manufacturer's instructions. Isolated B cells exhibited >99.5% viability confirmed by trypan blue exclusion and >95% purity by flow cytometry. Cells were further purified by cell sorting using a FACSAria (BD Biosciences). A representative sample of human B cell subsets is shown in Fig. 1*A*. Cells were stained with PE-Cy5-conjugated anti-hCD3, -hCD4, -hCD8, -hCD11b, -hCD14, -hCD56, -human glycophorin A; FITC-conjugated anti-human IgG; FITC-conjugated anti-human IgA; and PE-conjugated anti-hCD27 to obtain naive ($IgG^-A^-CD27^-$), IgM^- memory ($IgG^-A^-CD27^-$), and switched memory (IgG^-/IgA^-CD27^-) B cells. Isolated B cell subsets exhibited >95% viability confirmed by trypan blue exclusion and >99% purity by flow cytometry (Fig. 1*B*). Cells were cultured at 1×10^6 cells/ml in a flat-bottom 96-well microtiter plate in complete RPMI 1640 supplemented with 10% FCS. Preliminary experiments showed that trace levels of phosphorylation of BCR signaling molecules are observed in B cell subsets immediately after purification probably due to mechanical stress. The cells were thus rested for a couple of hours and used for further analysis throughout the study. Consistent with a previous study (2), IgM^+ memory B cells exhibited a slightly higher level of IgM and a slightly lower level of IgD than did naive B cells (Fig. 1*C*). Absence of surface expression of CD95, CD86, and CD69, representative activation markers, in both subsets before stimulation, suggests that these cells are rested (Fig. 1*C*).

Expression constructs and transient transfection of human B subsets

Constructs encoding human Tcl1- or Gal-1-enhanced GFP (EGFP) fusion proteins (pEGFP-Tcl1 or -Gal-1) were generated by inserting sequence encoding the full-length protein into the pEGFP-N3 vector (Clontech). Transient transfections of B cell subsets with pEGFP-Tcl1 or pEGFP-Gal-1 were conducted using the Nucleofector protocol from AMAXA Biosystems. Cells (1×10^6) were suspended in 100 μl of Nucleofector solution with 5 μg of plasmid DNA and then electroporated using program U-15. Cells were transferred to 2.5 ml of medium containing 15% FCS and harvested 24 h after transfection. The transfection efficiency ranges between 20 and 30% for each experiment.

Annexin V staining

After culture, cells ($1–2 \times 10^5$) were washed twice with PBS and then suspended in 85 μl of binding buffer (MBL) containing Ca^{2-}. Cell suspension supplemented with 10 μl of annexin V-FITC or -PE (MBL) and 5 μg of propidium iodide or 1 μg of 7-aminoactinomycin D was incubated at room temperature for 15 min in the dark. Subsequently, 600 μl of binding buffer were added, and the percentage of early apoptotic cells was measured using flow cytometry.

Mitochondria membrane potential

Assessment of mitochondria membrane potential was performed using Mitotracker Red CMXRos (Invitrogen). Cells were incubated in 50 nM Mitotracker Red at 37°C for 1 h in the dark. Flow cytometric analysis (50,000 events/sample) was performed on FACSCalibur (BD Biosciences). Cell debris was electronically gated out based on the forward scatter. Data were further analyzed using FlowJo software.

Measurement of intracellular free calcium

Cells were washed with RPMI 1640 containing 10% FCS and adjusted at 1×10^6 cells/ml. After incubation at 37°C for 15 min, 1 μg/ml fluo-4-acetoxymethyl esterM (Dojindo) was added, and the cells were incubated for a further 30–45 min with resuspension every 15 min. The cells were centrifuged and resuspended in RPMI 1640 at 2×10^5 cells/ml. The cells were stimulated with anti-IgM (20 μg/ml), and the fluorescence intensity of intracellular fluo 4 was monitored and analyzed using flow cytometry.

Western blot analysis

Unstimulated or stimulated cells (1×10^6) were lysed as described (13). Lysates were then denatured in an equal volume of 2× SDS sample buffer, resolved by a 10% SDS-PAGE gel and electrotransferred to nitrocellulose membranes in non-SDS-containing transfer buffer (25 mM Tris, 0.2 M glycine, 20% methanol, pH 8.5). Western blotting was performed with anti-phospho-Syk (1/2,000), anti-phospho-PLCγ2 (1/2,000), anti-phospho-p85/p70 S6 kinase (1/2,000), anti-phospho-JNK (1/2,000), anti-phospho-ERK (1/2,000), anti-phospho-Akt (1/2,000), anti-phospho-p65 NF-κB (1/2,000), anti-Bim (1/2,000), anti-Bcl-x_L (1/2,000), anti-Mcl-1 (1/5,000), anti-Tcl1 (1/2,000), anti-Gal-1 (1/2,000), and anti-β-actin (1/5,000) followed by a 1/15,000 dilution of anti-rabbit or anti-mouse HRP-conjugated IgG (Jackson ImmunoResearch Laboratories). Blots were developed with ECL plus kit (Amersham Biosciences). The chemiluminescence intensity was monitored with a laser3000 (FujiFilm) instrument. We quantitated band intensity of the proteins using ImageGauge software (FujiFilm) and normalized their expression in reference to β-actin levels. Using these normalized data, relative expression is subsequently calculated as fold changes in protein expression compared with the controls.

Quantitative real-time PCR

Total RNA was extracted from sorted human B cell subsets using Isogen reagent (Nippon Gene) and treated with DNase I (Invitrogen) to remove contaminating genomic DNA. First-strand cDNA was synthesized using a

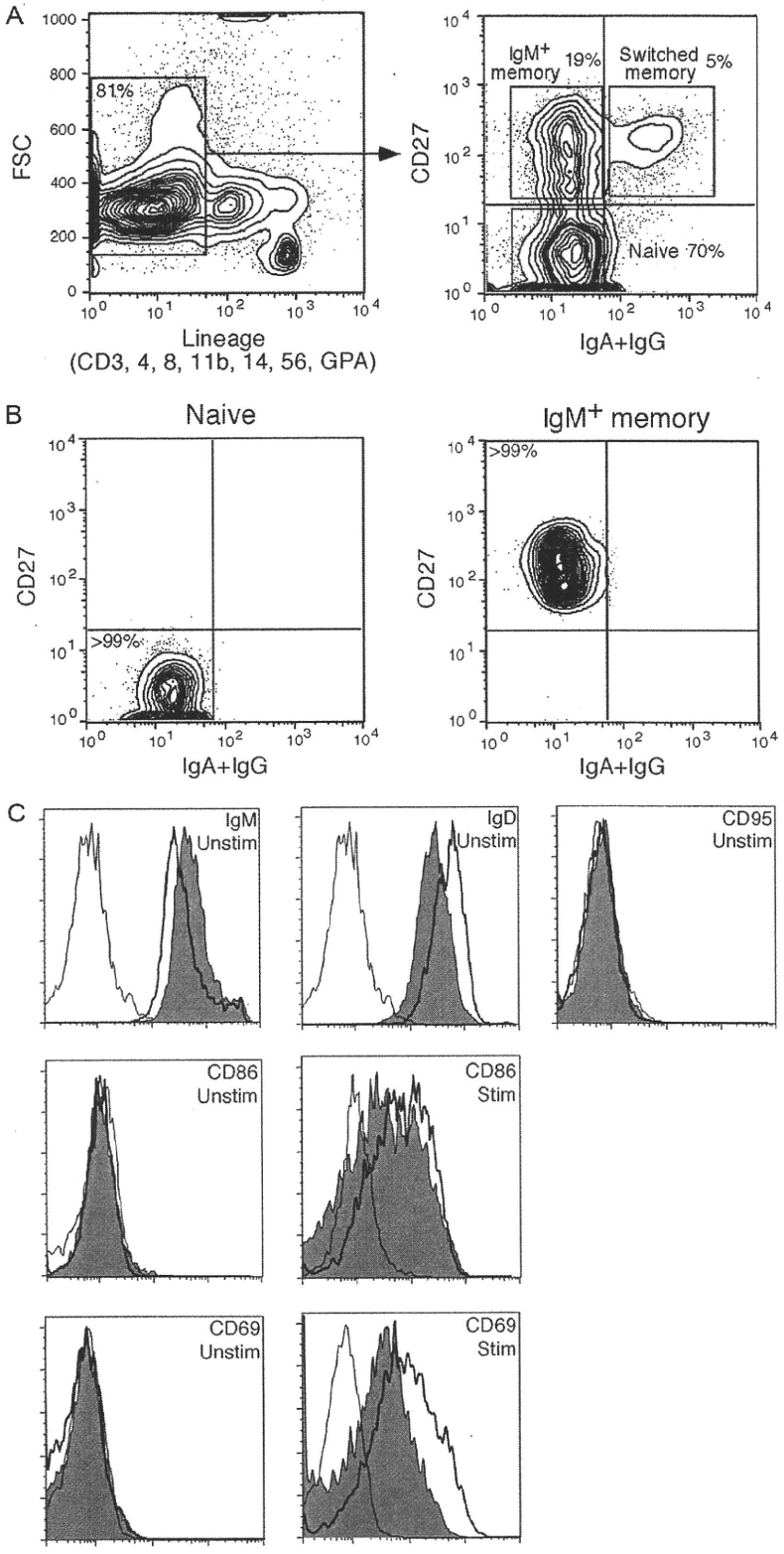

FIGURE 1. Isolation of purified human peripheral B cell subsets. *A*, Phenotypic analysis of B cell subsets in human peripheral blood. Donor B cells were purified by staining with Abs to CD3, CD4, CD8, CD11b, CD14, CD56, and glycophorin A (GPA) and were then evaluated by flow cytometry. B cell subsets were identified according to surface IgG/IgA and CD27 expression: $IgG^-A^-CD27^-$ B cells (naive), $IgG^-A^-CD27^+$ B cells (IgM^+ memory), and $IgG^+A^+CD27^+$ B cells (switched memory). Data are presented as density plots. *B*, Highly purified B cell subsets were separated after cell sorting. *C*, Surface marker expression in human B cell subsets. Purified B cell subsets before (Unstim) and after stimulation (Stim) with 20 μg/ml $F(ab')_2$ goat anti-hIgM (36 h) were analyzed separately for IgM, IgD, CD95, CD86, and CD69 surface expression. Bold line, Naive B cells; gray area, IgM^- memory B cells; thin line, isotype control line. These results are representative of peripheral blood samples from more than 10 different donors.

QuantiTect reverse transcription kit (Qiagen). Quantitative real-time PCR was conducted in the ABI Prism 7700 Sequence Detector (Applied Biosystems). Reactions were performed in triplicate wells in 96-well plates. TaqMan target mixes for Bim, Bcl-x_L, Mcl-1, Tcl1, and Gal-1 were purchased from Applied Biosystems. 18S rRNA was separately amplified in the same plate to be used as an internal control for variances in the amount of cDNA in PCR. Collected data were analyzed with Sequence Detector software (Applied Biosystems). Data were expressed as a fold change in gene expression relative to those from unstimulated naive B cells.

Intracellular flow cytometry

After two washings with PBS containing 1% FCS, 5×10^5 cells were placed in a 96-well microtiter plate. Cells were resuspended with 50 μl of medium plus 50 μl of fixation buffer (BD Biosciences) and incubated for 10 min at 37°C. After washing again with PBS containing 1% FCS, cells were suspended with 50 μl of saponin permeabilization buffer (BD Biosciences) and spun down. The cell pellet was incubated with primary Abs (anti-human Mcl-1 or Bim) in saponin buffer at room temperature for

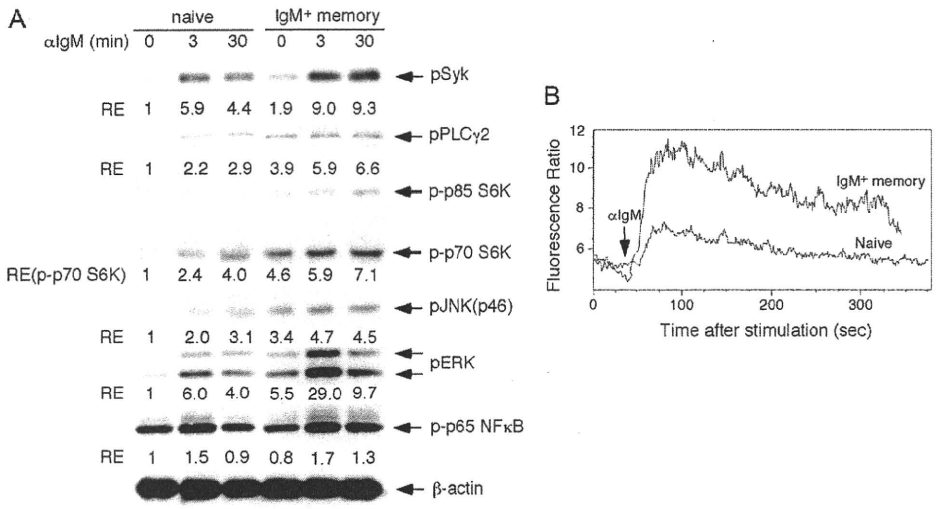

FIGURE 2. BCR signaling profiles of naive and IgM$^-$ memory B cells at early time points. *A*, B cell subsets were stimulated with 20 μg/ml F(ab')$_2$ goat anti-hIgM for the indicated time intervals. Cell lysates were subsequently separated on an 8% or 10% SDS-PAGE gel, and analyzed by Western blotting with anti-phospho-Syk, -PLCγ2, -JNK, -ERK sera, and anti-phospho-p70/85 S6K, -p65 NF-κB mAb and anti-β-actin mAb. Results are representative of three independent experiments. RE, Relative expression. *B*, Ca^{2+} mobilization in naive and IgM$^-$ memory B cells. Intracellular free calcium levels in fluo-4-acetoxymethyl ester-loaded cells were monitored using flow cytometry, after cells were stimulated with 20 μg/ml F(ab')$_2$ goat anti-hIgM. Results are representative of five independent experiments.

30–45 min. After a washing with PBS containing 1% FCS, cell were incubated with PE-conjugated donkey anti-rabbit IgG (Jackson Immuno-Research Laboratories) at room temperature for 30–45 min. Cells were washed one more time with PBS containing 1% FCS and analyzed at low flow rate on a FACSCalibur. B cell population was identified on its forward and side scatter distribution, and 15,000 cell events were analyzed for mean fluorescence using FlowJo software.

Results

Early BCR signaling is exaggerated in IgM$^+$ memory but not naive B cells

BCR signaling is critical for B cell fate decisions such as B cell survival, growth, and differentiation (14). We first tested whether the profile of early BCR signaling is different between naive and IgM$^+$ memory B cells. Phosphorylation of Syk, one of the earliest events in BCR signaling, was more pronounced in IgM$^+$ memory B cells (Fig. 2*A*). Two enzymes, PI3K and PLCγ2, function as critical mediators downstream of Syk activation in B cells (15). Phosphorylation of p85/p70 S6K, a downstream molecule of PI3K, and PLCγ2, was more pronounced in IgM$^-$ memory B cells (Fig. 2*A*). Activated PLCγ2 converts phosphatidylinositol 4,5-bisphosphate into IP3 and diacyl glycerol, the former of which is critical for calcium flux in B cells (14). Consistent with PLCγ2 phosphorylation, BCR-induced calcium flux was higher in IgM$^+$ memory B cells (Fig. 2*B*). Calcium flux and diacyl glycerol led to activation of NF-κB and MAPKs such as JNK and ERK. Phosphorylation of JNK and ERK was more pronounced in IgM$^+$ memory B cells, whereas p65 NF-κB phosphorylation was comparable in both subsets (Fig. 2*A*). Taken together, during the early phase of BCR activation, downstream signaling is pronounced especially in IgM$^+$ memory B cells as compared with naive B cells.

BCR stimulation rescues naive but not IgM$^+$ memory B cells from apoptosis

Following anti-IgM stimulation alone, naive and IgM$^+$ memory B cells did not either divide or release Igs in the culture (data not shown), suggesting that BCR signaling alone is not sufficient to induce the growth and differentiation of human B cell subsets. We then tested whether the BCR signaling affects the survival and death of naive and IgM$^+$ memory B cells. In the absence of stimuli, a considerable fraction of purified naive and IgM$^+$ memory B cells underwent apoptotic cell death within 2 days in vitro (Fig. 3*A*). Spontaneous cell death was more pronounced in naive B cells than in IgM$^+$ memory B cells. BCR stimulation, however, significantly rescued naive B cells from apoptosis, whereas IgM$^+$ memory B cells were not rescued (Fig. 3, *A* and *B*). Thus, BCR signaling can protect naive, but not IgM$^+$ memory B cells from apoptotic cell death.

Mitochondrial perturbations including cytochrome *c* release and inner membrane depolarization correlate with BCR-induced apoptosis (16). We thus tested whether BCR-induced depolarization of the mitochondrial inner membrane could be altered in naive and IgM$^+$ memory B cells. High levels of mitochondrial membrane potential were observed in both subsets immediately after sorting, indicating their highly viable state (Fig. 3*C*, *a* and *d*). A 2-day culture of these subsets without stimuli caused a remarkable decrease in mitochondrial membrane potential (Fig. 3*C*, *b* and *e*). BCR stimulation for 2 days, however, partially abrogated the loss of mitochondrial membrane potential in naive, but not IgM$^+$ memory B cells (Fig. 3*C*, *c* and *f*). Thus, BCR signaling rescues the B cell apoptosis pathway upstream of mitochondrial damage in naive, but not IgM$^+$ memory B cells.

BCR stimulation induces anti-apoptotic Mcl-1 in naive B cells, whereas it induces proapoptotic Bim in IgM$^-$ memory B cells at the protein level

Bcl-2 family proteins are the primary regulators of mitochondrial membrane integrity and play a vital role in the control of apoptosis (9). We tested whether BCR signaling affects gene expression of Bim, Bcl-x_L, and Mcl-1 in naive and IgM$^+$ memory B cells (Fig. 4*A*). Bcl-x_L mRNA expression was induced after BCR stimulation in both subsets, and such induction was more pronounced in naive B cells. In contrast, the expression level of Bim mRNA was slightly higher in IgM$^+$ memory B cells irrespective of BCR stimulation. Mcl-1 mRNA expression was not significantly changed in both subsets. We next tested whether BCR signaling affects protein